WETTABILITY OF ALUMINIUM WITH ALUMINIUM CARBIDE (GRAPHITE) IN ALUMINIUM FILTRATION

Sarina Bao[1], Kai Tang[2], Anne Kvithyld[2], Thorvald Abel Engh[1], Merete Tangstad[1]
[1]Norwegian University of Science and Technology, Trondheim, NO-7491, Norway
[2]SINTEF Materials and Chemistry, Trondheim, N-7465, Norway

Keywords: Wettability, Contact angle, Aluminium, Graphite, Al_4C_3, Time dependent property

Abstract

Graphite filters have previously been employed based on petrol coke. Wetting between molten aluminium and graphite is studied. Al_3C_4 is formed at the interface between aluminium and graphite. In filtration of aluminium inclusions such as Al_3C_4 formed in the hall electrolysis are removed. Wetting between aluminium and Al_3C_4 (graphite) is determined in kinetic studies in the higher temperature range 1000-1200°C. The results are extrapolated down to temperatures employed in the industry around 700°C. The contact angle between aluminium and graphite decreases with time. It may be divided into three stages: removal of an oxide layer on aluminium, formation of Al_3C_4 at the interface, finally giving an equilibrium value for Al-Al_3C_4. This value is found to be around 126° at 700°C.

Introduction

Carbon filters have been industrialized as petrol coke filter-DUFI during 1970-1985, known for removing hydrogen, alkaline metals and non-metallic inclusions in plants operated by the ALUSUISEE Group and elsewhere [1]. Al_3C_4 is formed at the interface between aluminium and graphite. In filtration of aluminium, inclusions such as Al_3C_4 formed in the hall electrolysis are removed. In this work, the wetting behaviour of Al-graphite system is investigated in order to answer the following two questions:

1. Can carbon be the new filter material choice again, due to changes in price of carbon and on requirements for cleanliness of metal?
2. What is the wetting behaviour between the Al_3C_4 inclusion and aluminium?

In the last decades, several studies had been devoted to the wetting behaviour of the Al-graphite system [2-4]. As a reactive wetting system, it was agreed that 1) the final or steady contact angle is equal or very close to the equilibrium contact angle of the liquid on the reaction product [2]; Tomsia et al. [6] found that the wetting behaviour of the reaction product is governed by the formation of adsorption layers at the interface, rather than by the subsequent nucleation and growth of the reaction product; 2) wettability would not be improved by the chemical reaction itself. The inter-atomic force is not correlated to the Gibbs free energy as an exchange of atoms is involved in a chemical reaction [3]. The Al-graphite system has the peculiarity that 1) the final contact angle, θ_2 on reaction product Al_4C_3 is much lower than the initial contact angle, θ_0 on the original substrate graphite; and 2) reaction product Al_4C_3 crystals are brittle and highly sensitive to moisture and thus promote accelerated fatigue crack growth rates in aluminium due to their hydrophilic nature [4].

The study of wettability of the Al-graphite system by the sessile drop technique gives rise to two main points. The first one is that liquid aluminium reacts with the graphite and forms Al_4C_3 at and close to the interface. Then wetting of the Al-graphite system is indeed the wetting of Al-Al_4C_3 system. The second one is that liquid aluminium is generally covered by an oxide layer which prevents it from wetting the substrate. The effect of this oxide layer on the wetting of Al- graphite system can be minimized if the pressure of system is lower than 10^{-8} bar and temperature is higher than 1000°C [5].

The wetting behaviour of the Al-graphite system in the temperature range 1000-1200°C under 10^{-8} bar vacuum is studied, and the wettability at aluminium casting temperature 700°C is then predicted. The contact angle initially changes with time and finally approaches "an equilibrium value". This time dependent characteristic is vital for understanding the mechanisms of aluminium filtration by graphite filters. The wettability of Al_4C_3 inclusions in liquid aluminium should be known to describe the inclusion removal.

Experimental Procedure

The contact angle of liquid aluminium on the graphite substrate was measured using the sessile drop technique. There are two typical sessile drop techniques reported in the literature. The first one uses contact heating — the metal and substrate are heated in contact and de-oxidation of the drop is attained by evaporation of the oxide layer; The second one applies capillary purification — the molten metal is dropped onto the substrate by extrusion through a graphite capillary which breaks the superficial oxide layer [6]. Since oxide layer exists in aluminium filtration, the contact heating method is used in this work.

The experimental apparatus using the sessile drop method is schematically shown in [7]. The apparatus essentially consists of a horizontal graphite heater surrounded by graphite radiation shields, located in a water-cooled vacuum chamber. The chamber was fitted with windows to allow a digital video camera (Sony XCD-SX910CR, Sony Corporation, Millersville, MD) to record the shape of the droplet. The contact angles and linear dimensions of the images were measured directly from the image of the drop using the Video Drop Shape Analysis software (First Ten Angstroms, Inc., Portsmouth, VA). We assume symmetry of the drop. After the experiments, no asymmetry was observed.

Drevet et al. [8] concluded that wetting kinetics is influenced by crystallographic factors of the substrate in Al- graphite system. Vitreous carbon, pyrolytic carbon, and graphite pseudo single crystals are studied in the literature [9]. In this work, experiments were carried out using the graphite (ISO-88) substrate and 99.999% pure aluminium. The average roughness of the graphite was 179.76nm. The aluminium rod with a

diameter of 2mm was cut into small pieces around 2mm in length, then polished by 500 mesh SiC paper and cleaned with ethanol in order to prevent further oxidation. The graphite substrate was dried in a furnace at 100°C before the measurement.

When the wetting furnace attained the high vacuum of 10^{-8} bar, the sample was quickly heated to 950°C in about 80s, then heated to 1000, 1100, and 1200 at the rate of 50°C/min, as shown in Figure 1. Although the furnace temperature overshoots to 1100°C at the first 80s, it does not affect the wettability at a lower temperature such as 1000°C, since the oxide skin holds the liquid metal at the beginning. In all of the experiments, the contact angle and dimensions of the drop were recorded during the isothermal period at 1000, 1100, and 1200 °C. Time=0 was taken to be the beginning of the isothermal period.
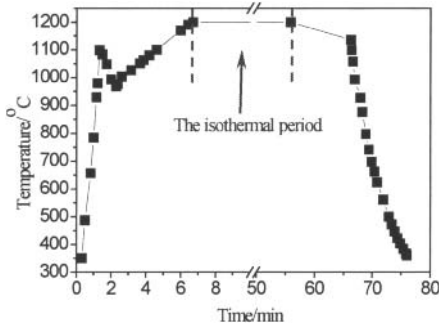
Figure 1 Example of the registered temperature for the experiment holding the sample at 1200 °C
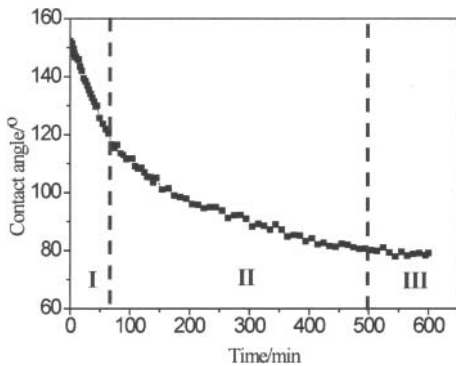
Results

Wettability between aluminium and graphite at 1000°C as the function of time is shown in Figure 2 and Figure 3. Three kinetic stages can be distinguished: the first stage, where the contact angle decreases rapidly (in 64 min) from the initial contact angle $\theta_0 \approx 152°$ to $\theta_1 \approx 120°$; the second stage where the contact angle continues to decrease to a relatively low value of $\theta_2 \approx 80°$, but at a slower rate; and the third stage where the contact angle stabilized at θ_2 after approximately 500 min. The stable base diameter and the sessile volume allow the stable contact angle in the third stage to be measured.

Similar three kinetic stages: (I) rapid decrease, (II) slow decrease and (III) stable contact angle at 1100°C are shown in Figure 4 and Figure 5. The stable base diameter and the sessile volume guarantee the stable contact angle in the third stage. A lower stable contact angle is obtained in a shorter time at 1100°C than at 1000°C (See Table I).

Efforts to obtain the Al-graphite contact angle at even higher temperatures, for example 1200°C, were made, as shown in Figure 6 and Figure 7. Unfortunately, the evaporation of aluminium at higher temperatures is so high that the aluminium droplet disappeared quickly.

Experimental results of aluminium on graphite are summarized in Table I.

Table I Results of aluminium on graphite

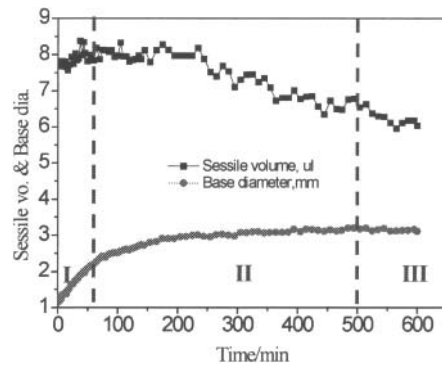| Tempe- rature	Stage.I	Stage.II		Stage.III	
	$\theta_0/°$	$\theta_1/°$	t_1/min	$\theta_2/°$	t_2/min
1000°C	152	120	64	80	500
1100°C	157	107	14	62	209

Figure 2 Contact angle at 1000°C

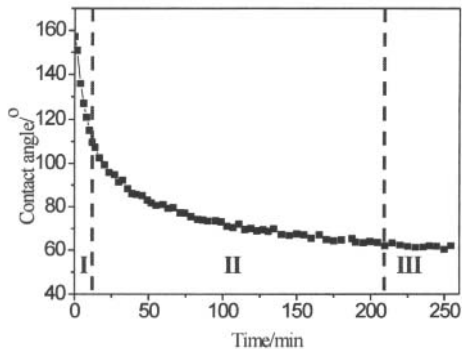Figure 3 Sessile volume and base diameter at 1000°C
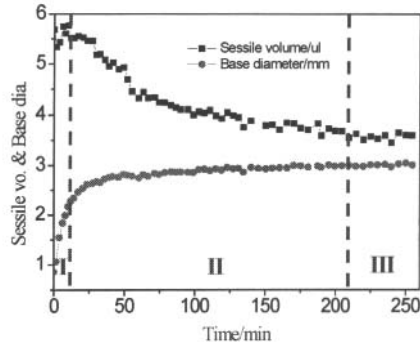
Figure 4 Contact angle at 1100°C

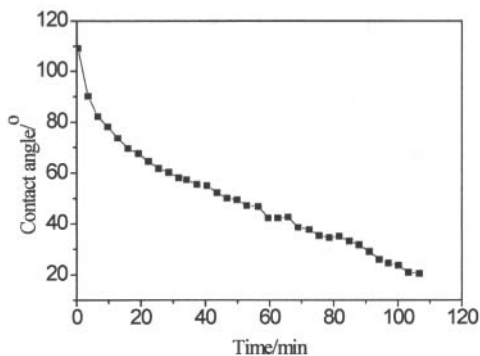Figure 5 Sessile volume and base diameter at 1100°C
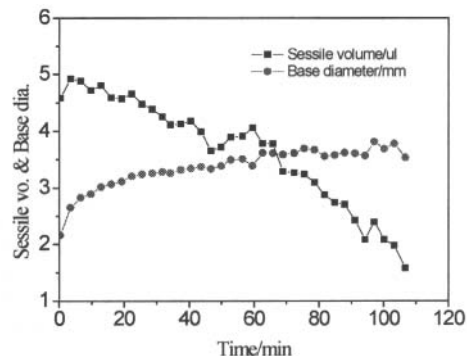

Figure 6 Contact angle at 1200°C

Figure 7 Sessile volume and base diameter at 1200°C

Figure 8 shows the presence of a continuous layer of reaction product, Al_4C_3 at the Al-graphite interface with a thickness of 130μm. The graphite-Al_4C_3 interface is rougher than the graphite substrate before the experiments and pores are present around some particles. Extra aluminium in the Al_4C_3 layer and the discrete Al_4C_3 particles indicates that the reaction proceeds by dissolution of carbon into aluminium. The final contact angle is determined by the Al-Al_4C_3 system.
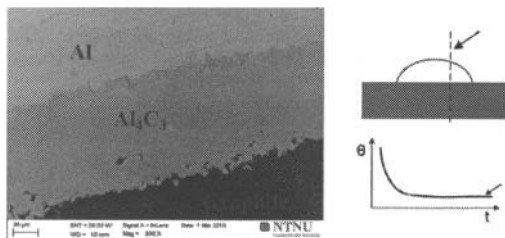

Figure 8 SEM micrograph of a cross section in an Al-graphite specimen cooled naturally after 250 min at 1100°C

Discussion

The three successive stages of wetting kinetics in Figure 2 to Figure 7 are discussed.

Stage.1- De-oxidation of oxide layer

The sharp decrease of the contact angle from θ_0 to θ_1 on the Al-graphite system is similar to the contact angle curve observed previously for Al-Al_2O_3 for the same stage in the same wetting furnace. This reduction is due to de-oxidation of the oxide layer according to reaction

$$4Al(l) + Al_2O_3 = 3Al_2O(g) \qquad (1)$$

This is effective when the outgoing flow of oxygen in Al_2O (g) is higher than the incoming flow of oxygen. The $P_{Total}=10^{-3}$ Pa (10^{-8} bar) in the furnace guarantees that P_{Al2O} is lower than the equilibrium $P_{Al2O}=3.7\times10^{-3}$ Pa at 1000°C [10]. Thus the wetting behaviour of the first stage is controlled by de-oxidation of the oxide layer on the aluminium drop.

Stage.II- Al_4C_3 formation

In the second stage from time t_1 to t_2 in Al-graphite system, the spreading velocity is lower than the previous stage and the base diameter is a linear function with respect to time. This second stage does not exist in the non-reactive Al-Al_2O_3 system [5]. The interfacial reaction (2) has Gibbs energy of -136kJ/mol to -102kJ/mol [11] at temperatures of 660 to 1300°C. The second

stage in Al- graphite system is controlled by the formation of Al_4C_3.

$$4Al(l) + 3C(s) = Al_4C_3 \qquad (2)$$

Stage.III- Stable contact angle

The Al- Al_4C_3 system is formed at the end of the second stage in which a relatively stable contact angle is detected in the third stage. Good repeatability experiments at the same temperature of wetting property were observed.

The contact angle initially changes with time and finally approaches an "equilibrium value". This system produces Al_4C_3 at the end and the interface reaction product promotes the wetting.

Empirical Calculation

The equilibrium value of the contact angle θ obeys the classical equation of Young:

$$\cos\theta = \frac{\sigma_{Al_4C_3} - \sigma_{inter}}{\sigma_{Al}} \qquad (3)$$

where σ_{Al4C3}, σ_{inter}, and σ_{Al} are the surface energies of Al_4C_3-vapour, Al_4C_3-Al, Al-vapour, respectively. We have not taken into account the effect of the curvature of the aluminium droplet [12, 13]. Most of the reported surface tension measurements pertain to "oxygen saturated" samples [14]. According to Mills and Su [14], the surface tension of oxygen saturated [14] molten aluminium can be evaluated:

$$\sigma_{Al} = 993.86 - 0.18T(^\circ C) \text{ in mN/m} \qquad (4)$$

Since the surface energy of Al_4C_3 has not been reported in the literature, one may use the value of σ_{Al4C3}-σ_{Inter} to estimate the contact angle at lower temperatures. Figure 9 shows the σ_{Al4C3}-σ_{Inter} values as a function of temperature. It is obvious that the experimental data can be divided into two sets: those of Landry using the vitreous graphite substrate, the present measurements and those of Landry using single- and ploy-crystal graphite.
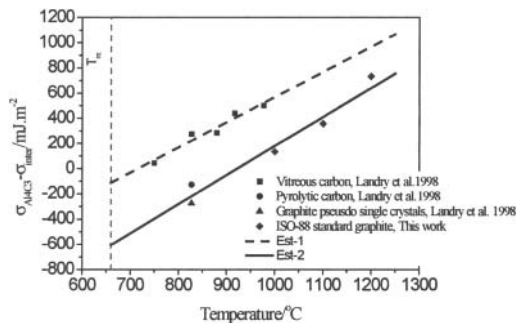

Figure 9 σ_{Al4C3}-σ_{inter} fitted to literature data [9] under 10^{-8} bar vacuum and this work

If we approximate the σ_{Al4C3}-σ_{Inter} values as a linear function of temperature, the contact angle of Al-Al_4C_3 system at casting temperatures can be estimated using the following equation:

$$\cos\theta = \frac{2.3T(^\circ C) - 2125.3}{\sigma_{Al}} \qquad (5)$$

for this work, where 2.3 is the slope of Est-2.

Figure 10 shows the calculated contact angle with the measured values at various temperatures. The contact angle between aluminium and Al_4C_3 (single- and ploy-crystal graphite) at 700°C is around 126°, which indicates that Al_4C_3 (graphite) is not wetted by molten aluminium at the casting temperature. If the vitreous graphite is used, the contact angle reduces to 92° at 700°C. This is reasonable due to the imperfectly crystallized form in vitreous graphite.
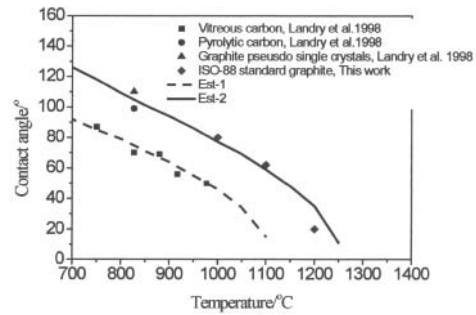

Figure 10 The calculated and measured contact angle vs. temperature for Al on various graphites

Eustathopoulos et al. [15] found out that spreading during the interfacial reaction can be described by

$$R - R_0 = Kt \qquad (6)$$

Where R_0 is the initial drop base radius at the start of the reaction and K is a system constant, independent of the drop volume. Figure 11 shows linear fitting of the base diameter in the second stage with fitting factor 92.6%. The experimental data in Figure 11 is a zoom of the second stage presented in Figure 5. The spreading rate of the triple line, K=d(diameter)/dt is equal to 1.53μm/min in the second stage at 1100°C. The spreading rates are 0.87μm/min and 7.46μm/min at 1000°C and 1200°C in the second stage.

The sessile volume shows evaporation rates of 4.21nL/min, 4.33 nL/min, and 28.39nL/min at 1000°C, 1100°C, and 1200°C in the second stage, respectively.

As suggested with Ambrose et al. [16], the decay of the contact angle with time can be fitted empirically by an exponential form:

$$\theta_t - \theta_2 = (\theta_0 - \theta_2)\exp(-t/\tau) \qquad (7)$$

where θ_t is the contact angle at time t and τ is a characteristic time factor.
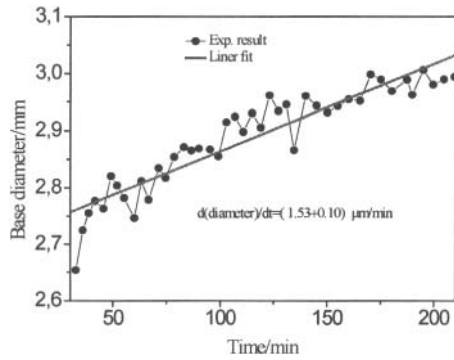
Figure 11 The base diameter vs. time at 1100°C

When θ_0, θ_2 and τ are known, the time dependent property of the Al-graphite system can be estimated at the casting temperature. The initial contact angle θ_0, is not significantly altered by a change of temperature [9] and substrate since all the wetting start from non-wetting, assuming $\theta_0=160°$. In this work, θ_0 is lower than 160° due to the several minutes holding before the time zero, as shown in Figure 1. As shown in Figure 10, $\theta_2=126°$ at 700°C.

The characteristic time factor τ seems related to the de-oxidation time which depends on oxygen partial pressure. This needs further investigation. However, when we take $\tau= 23$ min (the lowest de-oxidation limit from the literature [17]), the time dependent wetting behaviour of Al-graphite system at 700°C can be predicted and shown in Figure 12. Note that τ changes the decreasing rate of the contact angle, but not the final equilibrium contact angle.
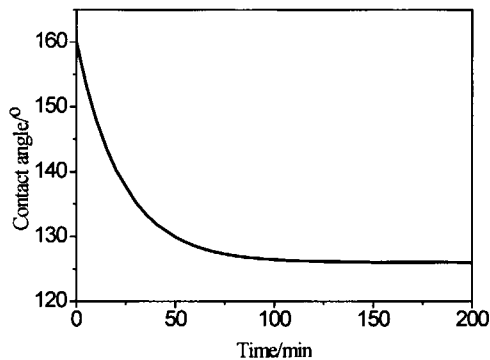

Figure 12 The simulation curve of the contact angle for Al on graphite at 700°C
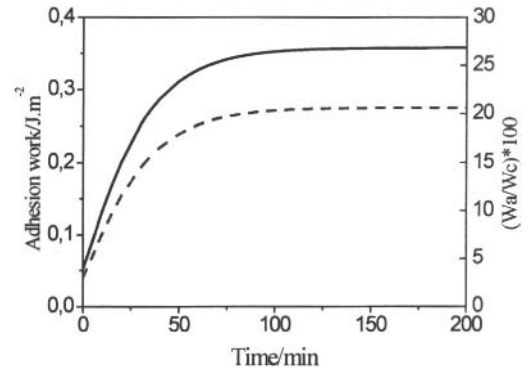


Figure 13 The adhesion work and the ratio Wa/Wc at 700 °C

The adhesion work W_a (see Equ.(8)) and ratio of that with cohesion work W_c (see Equ.(9)) at 700°C are shown in Figure 13. It shows that adhesion (attraction to dissimilar molecular) work is less than 25% of the work of cohesion liquid aluminium. This indicates that the $Al-Al_4C_3$ (graphite) interface is energetically weak, which is due to covalent bonds of Al_4C_3[6].

$$W_a = \sigma_{LV}(1+\cos\theta) \qquad (8)$$
$$W_c = 2\sigma_{LV} \qquad (9)$$

The final contact angle is the contact angle between Al_4C_3 and aluminium. Al_4C_3 (2.36g/cm^3 density, 0.5-25μm dimension) is one of the most common inclusions in aluminium. The Al_4C_3 particles have been present in liquid aluminium for a long time before filtration. Therefore the contact angle of Al_4C_3 particles and aluminium is believed to be constant 126° and the adhesion work is 357.8mJ/m^2. Al_4C_3 is not wetted by aluminium and it can be removed readily if aluminium wets with the filter material.

Al_4C_3 reacts with water vapour according to reaction:

$$Al_4C_3 + 12H_2O = 3CH_4 + 4Al(OH)_3 \qquad (10)$$
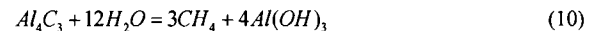
Release of methane and Al_4C_3 may be a reason not to use graphite as a filter in an industry environment.

Conclusions

1. The wetting behaviour of the Al-graphite system at temperature 1000-1200°C under 10^{-8} bar vacuum was investigated and the contact angle was extrapolated to the casting temperature 700°C. The equilibrium contact angle is 126° at 700°C for the Al -Al_4C_3 (graphite) system.
2. The wettability of the Al-graphite with respect to time can be divided into three kinetic stages: (I) de-oxidation of alumina layer, (II) Al_4C_3 formation at the interface, and (III) the stable contact angle.
3. Due to the poor wetting between Al_4C_3 and molten aluminium at casting temperature, Al_4C_3 inclusions can be captured by other filter materials having better wettabilities with liquid aluminium.

4. The hydrophilicity and Al_4C_3 may be problems to use graphite as a filter material.

References

1. Bornand, J.-D. and K. Buxmann, *DUFI: A Concept of Metal Filtration.* Light Metals, 1985: p. 1249-1260.
2. Kalogeropoulou, S., C. Rado, and N. Eustathopoulos, *Mechanisms of reactive wetting: the wetting to non-wetting case.* Scripta Materialia, 1999. **41**(7): p. 723-728.
3. Zhou, X.B. and J.T.M.D. Hosson, *Reactive wetting of liquid metals on ceramic substrates.* Acta Materialia, 1996. **44**(2): p. 421-426.
4. Etter, T., et al., *Aluminium carbide formation in interpenetrating graphite/aluminium composites.* Materials Science and Engineering A, 2007. **448**(1-6).
5. Bao, S., et al., *Wettability of Aluminium on Alumina.* Metallurgical and Materials Transactions B, 2011(DOI:10.1007/s11663-011-9544-z).
6. Landry, K., et al., *Characteristic contact angles in the Aluminium/vitreous carbon system.* Scripta Materialia, 1996. **34**(6): p. 841-846.
7. Bao, S., et al., *Wetting of Pure Aluminium on Filter Materials Graphite, AlF_3 and Al_2O_3.* Light Metals, 2009: p. 767-773.
8. Drevet, B., et al., *Influence of substrate orientation on wetting kinetics in reactive metal/ceramic systems.* Scripta Materialia, 1996. **35**(11): p. 1265-1270.
9. Landry, K., S. Kalogeropoulou, and N. Eustathopoulos, *Wettability of carbon by aluminum and aluminum alloys. Materials Science and Engineering: A,* 1998. **254**(1-2): p. *99-111.*
10. Standards, N.B.O., *JANAF Termochemical Tables, 2nd edition.* 1971. **37**.
11. Isaikin, A.S., et al., *Compatibility of Carbon Filaments with A Carbide Coating and an Aluminium Matrix.* Sci. Heat Treatment, 1980. **22**: p. 815-817.
12. Gaydos, J. and A. Neumann, *The Dependence of Contact Angles on Drop Size and Line Tension.* Journal of Colloid and Interface Science, 1987. **120**(1): p. 76-86.
13. Zhang, L. and S. Taniguchi, *Fundamentals of Inclusion Removal from Liquid Steel by Bubble Flotation.* International Materials Reviews, 2000. **45**(2): p. 59-82.
14. Mills, K.C. and Y.C. Su, *Review of surface tension data for metallic elements and alloys: Part 1 Pure metals.* International Materials Reviews, 2006. **51**(6): p. 329-351.
15. Eustathopoulos, N., J.P. Garandet, and B. Drevet, *Influence of reactive solute transport on spreading kinetics of alloy droplets on ceramic surfaces.* Philosophical Transactions of the Royal Society London A, 1998. **356**(1739): p. 871-884.
16. Ambrose, J.C., M.G. Nicholas, and A.M. Stoneham, *Dynamics of Braze Spreading.* Acta Metallurgica et Materialia, 1992. **40**(10): p. 2483-2488.
17. Laurent, V., D. Chatain, and N. Eustathopoulos, *Wettability of SiC by aluminium and Al-Si alloys* Journal of Materials Science, 1987. **22**(1): p. 244-250.